Published in final edited form as:
Ocul Surf. 2026 April 01; 40: 31–39. doi:10.1016/j.jtos.2026.01.007.

Lacrimal gland duct obstruction and dacryops: Unravelling its pathogenesis with proteomics and cellular profiling

Swati Singh[a,b,*]

[a]Hariram Motumal Nasta & Renu Hariram Nasta Ophthalmic Plastic Surgery Services, KAR Campus, LV Prasad Eye Institute, Hyderabad, Telangana, India.

[b]Prof. Krothapalli Ravindranath Ophthalmic Research Biorepository, LV Prasad Eye Institute, Hyderabad, Telangana, India.

Abstract

Purpose: To understand the pathogenesis of the main lacrimal gland dacryops (ductular cyst) using proteomics and cellular profiling.

Methods: Four patients (mean age, 42.2 ± 18.4 years) with dacryops underwent cyst excision following the aspiration of the cyst contents. Cyst contents were processed using mass spectrometry and compared with eight healthy tear samples. The cyst wall was processed for histology (H&E, Masson trichrome), epithelial (Aquaporin 5, CK15, CK19), stromal (Vimentin), neural (beta-III tubulin, NCAM), and immune cell markers (CD3, CD20, CD138, myeloperoxidase, CD68).

Results: The cyst lining was cuboidal to squamous in three cases (CK19+, ductal origin), and exhibited goblet cell metaplasia in one case. Compared to normal ducts, the dacryops cyst wall lacked expression of AQP5 and beta-III tubulin. Subepithelial fibrosis and strong vimentin positivity were observed in all specimens, along with mild to moderate inflammation. Infiltrating immune cells were $CD20^{+}$ and CD138+, with a few macrophages and neutrophils noted perivascularly. The visible few lacrimal gland acini within the cyst wall showed inflammation, IgA-positive plasma cells, and focal acinar atrophy. The cyst fluid and tear samples were widely separated on the PCA plot, with 190 proteins upregulated and 52 downregulated. The upregulated proteins were involved in immunoglobulin-mediated immune responses, complement activation, apolipoproteins, extracellular matrix components (including matrix metalloproteinases 7 and 10), and glycosaminoglycan binding.

Conclusion: Dacryops involves reactive ductular ectasia secondary to inflammation, resulting in increased MMPs, fibrosis, and loss of the periductal neural network. The cyst fluid is rich in apolipoproteins, immunoglobulins, and complement factors. Future research could focus on the lipidomics of the cyst fluid.

[*]L V Prasad Eye Institute Road No.2, Banjara Hills, Hyderabad, 500034, Telangana, India. swatisingh@lvpei.org, dr.swati888@yahoo.com.

Appendix A. Supplementary data

Supplementary data to this article can be found online at https://doi.org/10.1016/j.jtos.2026.01.007.

Europe PMC Funders Author Manuscripts

Keywords

Dacryops; Lacrimal gland; Tears; Proteomics; Duct

Europe PMC Funders Author Manuscripts

1 Introduction

Dacryops denotes cystic lesions within the main or accessory lacrimal glands, representing 3–17 % of all lacrimal gland lesions [1–7]. Patients with dacryops originating from the main lacrimal gland typically present with eyelid swelling, with or without pain [1–8]. Clinical examination can readily identify the diagnosis, which appears as a cystic, nontender lesion within the palpebral lobe of the main lacrimal gland [6,9]. The treatment is surgical, with a low recurrence rate [10–14]. However, the etiopathogenesis has been a subject of research for decades [6]. Dacryops represents cystic dilatation of the secreting ductules secondary to duct obstruction. The reported histological changes include double-layered cystic epithelium, variable fibrosis of the cyst wall, and inflammatory cells in the subepithelium [3,6]. Biochemical analysis of the cystic fluid from the accessory gland dacryops has reported elevated IgA levels [2,3]. The proposed theories revolve around ductal obstruction leading to mechanical dilatation, IgA-mediated osmotic gradient, conjunctiva-associated-lymphoid tissue (CALT) mediated periductal inflammation, hypersecretion, impaired neural reflex, or a combination [2–4,6]. However, in animal models, lacrimal gland duct obstruction does not result in cyst formation [15]. However, the aged mice's lacrimal glands have shown cysts that were found to be lipoid bodies on histological studies [27]. The composition of the dacryops cyst fluid in humans is unknown. The current investigation focuses on the main lacrimal gland dacryops, examining the proteomics of cyst fluid and the dacryops' epithelial, neural, immune, and mesenchymal cell profiles. Also, the outcomes of simple needling procedure (based on the proposed pathogenesis in the current study) for managing dacryops are discussed.

2 Methods

Consecutive patients with dacryops presenting to the tertiary eye center who were surgically managed over 1.5 years by a single surgeon (S.S) were included. The study adhered to the tenets of the Declaration of Helsinki, and the institutional review board approval was obtained. Routine surgical consent was obtained for the procedure. Demographic data, clinical details, and tissue blocks were analyzed. Histological staining included routine Hematoxylin & eosin (H&E) staining and immunostaining for epithelial (Aquaporin 5, CK15, CK19), stromal (Vimentin), neural (β III tubulin, neural cell adhesion molecule (NCAM) and immune cell profiling (CD3, CD20, CD11b, CD68, myeloperoxidase (MPO)). These antibodies were selected based on earlier studies on dacryops [4–7]. The cyst wall features were compared with those of the normal lacrimal duct. The proteomics of cyst fluid was measured using mass spectrometry. Schirmer strips were collected from healthy volunteers (n = 6) and hospital staff with no ocular or systemic disease to compare tear proteomics with cyst fluid. Three healthy lacrimal gland biopsies obtained from patients (mean age: 49 years; two males) undergoing gland debulking surgery were also immunostained with anti-bodies for comparison [16].

2.1 Surgical technique

Under local infiltration into the temporal upper eyelid and canthal region, the cyst was exposed by manually retracting the upper eyelid. Westcott scissors were used to give an incision at the junction of the cyst and adjacent healthy conjunctiva. Tissue undermining was done to expose the anterior face of the cyst. Cyst contents were aspirated using a 29-G needle attached to a 1 mL insulin syringe. After deflation, the posterior extent of the cyst could be easily seen, and the cyst wall was excised without damaging the adjacent uninvolved lacrimal gland lobules. The fluorescein dye-impregnated strip was used to localize the patent ductular opening, thereby avoiding damage. No electrocautery was used in any of the cases. Hemostasis was secured using pressure. Aspirated cyst content was stored immediately at &80° C.

2.2 Immunofluorescence

The earlier published protocol was used for immunostaining [17]. The antibody dilutions are available in Supplementary Table 1. Briefly, deparaffinized sections were rehydrated, followed by antigen retrieval and slide incubation with bovine serum albumin (catalog no. A7906, Sigma, USA) to avoid non-specific antibody reaction. The primary antibodies were applied for 1 h at room temperature (Suppl. Table 1). Slides were washed and incubated with fluorescent-tagged secondary antibodies for 45 min at room temperature in the dark-Alexa Fluor 594 anti-mouse IgG (1:400, Invitrogen, USA), Alexa Fluor 594 anti-rabbit IgG (1:400, Invitrogen, USA), and counterstained with DAPI. Images were captured using ZEISS Axio Scope A1 (Carl Zeiss, Germany). Inflammatory cell infiltration was graded as mild (few scattered cells or <25 cells/HPF), moderate (25–50 cells/HPF), and severe (>50 cells/HPF). Other antibodies' expression was defined as location and intensity - weak, moderate or strong compared to respective controls (Supplementary Fig. 1). Fibrosis percentage area was calculated from Masson Trichrome-stained images using Image J and the color deconvolution2 plugin.

2.3 Tear proteomics

Aspirated cyst content proteomics (mean volume 1.4 ± 0.3 ml) was compared with tear fluid collected using Schirmer strips from healthy individuals (n = 6, 34.7 ± 2.9 years, 4 males). Proteins extracted from Schirmer strips were eluted using a buffer containing 0.5 M NaCl and 1 % SDS followed by acetone precipitation. The precipitated proteins and tissue aspirates were resuspended in 50 mM Tris-Cl buffer at pH 8, supplemented with protease inhibitors. The protein sample was first reduced with 5 mM TCEP and then alkylated with 50 mM iodoacetamide. The protein was then digested with Trypsin at a 1:50 Trypsin-to-lysate ratio for 16 h at 37 °C. After digestion, the mixture was purified using a C18 silica cartridge and then concentrated by drying in a speed vacuum. The resulting dried pellet was resuspended in buffer containing 2 % acetonitrile and 0.1 % formic acid.

2.3.1 Mass spectrometric analysis of peptide mixtures: For mass spectrometric analysis, all the experiments were performed on an Easy-nLC-1000 system (Thermo Fisher

Conflict of interest
No conflicts exist for any of the authors.

Scientific) coupled with an Orbitrap exploris 240 mass spectrometer (Thermo Fisher Scientific) and equipped with a nano-electrospray ion source. 1 μg of the digested peptides sample was dissolved in buffer A containing 2 % acetonitrile/0.1 % formic acid and resolved using a Picofrit column (1.8 μm resin, 15 cm length). Gradient elution was performed with a 0–38 % gradient of buffer B (80 % acetonitrile, 0.1 % formic acid) at a flow rate of 500 nl/min for 96mins, followed by 90 % of buffer B for 11 min and finally column equilibration for 3 min. Orbitrap Exploris 240 was used to acquire MS spectra under the following conditions: Max IT = 60 ms, AGC target = 300 %; RF Lens = 70 %; R = 60K, mass range = 375–1500. MS2 data were collected under the following conditions: Max IT = 60 ms, R = 15 kV, AGC target = 100 %. MS/MS data were acquired using a data-dependent top 20 method, dynamically choosing the most abundant precursor ions from the survey scan, with dynamic exclusion employed for 30 s.

2.3.2 Data processing: RAW files were analyzed with Proteome Discoverer (v2.5) against the Uniprot reference database of Human. For dual Sequest and Amanda search, the precursor and fragment mass tolerances were set at 10 ppm and 0.02 Da, respectively. The protease used to generate peptides, i.e., enzyme specificity, was set for trypsin/P (cleavage at the C terminus of “K/R: unless followed by “P”). Carbamidomethyl on cysteine as a fixed modification and oxidation of methionine and N-terminal acetylation were considered as variable modifications for database search. Both peptide spectrum match and protein false discovery rate were set to 0.01 FDR. Bar diagrams were created using the Mann-Whitney test in GraphPad Prism v.10 (USA) for the top relevant proteins. A correlation matrix was used to understand the association between cyst size and the top upregulated proteins. The Pearson correlation test was used to assess the correlation between disease duration and the area of fibrosis or inflammatory cell infiltration.

2.3.3 Dacryops needling: Based on our study results, the subsequent dacryops patients underwent cyst fluid release using a 26-G needle under topical anesthesia, 0.5 % proparacaine, on a slit-lamp. Needle puncture of the cyst released the fluid, and the cyst flattened out. Two cases were managed using needle aspiration over nine months. The palpebral lobe of the lacrimal gland was imaged before and after the procedure. Postoperatively, patients were given 0.5 % loteprednol etabonate (Lotepred, Sun Pharmaceuticals, India) eye drops for one week.

3 Results

3.1 Clinical details

Four patients (42.2 ± 18.4 years, three males) with unilateral dacryops were included. The main complaints were palpable upper eyelid canthal lesions, pain, and eye irritation (Fig. 1). The average cyst duration was 5.3 ± 1.4 months. The maximum mean cyst diameter was 9.2 ± 3.1 mm. All patients opted for surgical excision at the primary visit and had recently used only topical antibiotic drops. At a mean follow-up of 16.3 months, no recurrences were noted. The mean change in Schirmer I was 3.2 mm. None of the patients had a Schirmer I value of less than 10 mm pre- or postoperatively. The stained antibody expression and glandular features are listed in Tables 1 and 2.

3.2 Histopathology findings

3.2.1 Epithelial cell profiling: In all specimens, the cyst wall epithelium was non-keratinizing, two-cell layers thick, and cuboidal to columnar, with focal areas of a single layer of flattened epithelial cells in cases 2 & 4 (Fig. 2). CK19 and CK15 expression was strong in all specimens. CK19 expression was present in all epithelial layers in all specimens. Only one case with multicolumnar epithelium showed a basal layer of CK15-positive cells in the epithelium (Fig. 2). Only case 3 had goblet cells (PAS positive) interspersed within epithelial cells (Fig. 3). The epithelium was thrown into folds as if a collapsed cystic cavity.

3.2.2 Immune cell profiling: All specimens exhibited inflammatory cell infiltration, primarily perivascular, in both the glandular and stromal regions. The inflammatory cell density ranged from mild (cases 2 & 3) to moderate (cases 1 & 4; Fig. 4). Inflammatory cell density and fibrosis showed a weak negative correlation ($r = –0.3$; $p = 0.69$), but it did not reach statistical significance. Inflammatory cells expressed CD20, myeloperoxidase, and CD68. All specimens were negative for CD3. There were CD138-positive mononuclear cells present in the subepithelial and glandular stroma in specimens (Fig. 4). IgA immunostaining was positive within the lacrimal gland acini stromal cells (likely plasma cells) but not within the cyst lining or subepithelial space (Fig. 5).

3.2.3 Lacrimal gland changes: Three specimens showed glandular acini in the cyst wall stroma (Fig. 5). Acini were arranged in clusters with pyramidal-shaped epithelial cells (CK 19 positive) surrounding a central lumen. In case 4, acini showed interspersed inflammatory cell infiltration and acinar atrophy, but no intralobular fibrosis. AQP5 expression was strong and positive in the acini but absent in the cyst wall lining. AQP5 was localized to the luminal side in case 3 only; in the other two cases, AQP5 showed cytoplasmic retention (Fig. 5).

3.2.4 Neural expression: β III tubulin positivity was observed in the stromal nerve fibers, and periacinar cells (Fig. 6). The periacinar expression was seen in stromal cells, identified by their cellular morphology—likely fibroblasts and endothelial cells (Fig. 6, case 1). Periacinar nerve fibers were also seen as β III tubulin-positive structures, typically thread-like (Fig. 6, normal). The cyst epithelium was negative for tubulin staining, except in case 4. NCAM expression was focal and limited to the interstitium in all specimens (Fig. 6). It was absent from the glandular parenchyma, which is not seen in normal glands [17]. Additionally, βIII tubulin and NCAM expression were absent in the subepithelial region of the cyst wall.

3.2.5 Stromal cells: The subepithelial plane had extensive fibrosis, which was seen as bright blue on Masson trichrome staining (Fig. 6). The extent of fibrosis was greater in specimens (cases 1,4) with moderate inflammatory cell infiltration. The correlation between dacryops duration and fibrosis ($r = 0.68$; $p = 0.31$) was weak and statistically insignificant. There was an increase in vimentin expression within the stromal, periacinar, and periductular cells (Fig. 6). The subepithelial region showed strong vimentin positivity

in the spindle-shaped fibroblasts, mononuclear inflammatory cells, and endothelial cells. Numerous capillaries were seen in the subepithelial space (Fig. 6).

3.3 Fluid proteomics

A comparison of cyst fluid versus tear proteomics revealed distinct clusters based on principal coordinate analysis (Fig. 7A). A negative correlation between the two was observed, as indicated by the heat map, which showed distinctly upregulated and downregulated proteins (Fig. 7B and C). There were 391 differently expressed proteins between cyst fluid and tears, with 190 upregulated and 52 downregulated (Fig. 7D; Table 3). GO pathway analysis identified upregulated proteins belonging to the immune system process, immune response, immunoglobulin-mediated immune response, complement activation (Fig. 8A). The downregulated proteins were related to metabolism, gluconeogenesis, hedgehog signaling, cell cycle, and G2/M phase transition (Supplementary Fig. 2). Uniquely expressed proteins present in cyst fluids of all four cases were immunoglobulin heavy chain variable region 3 (IGHV3), lambda variable chain (IGLV3), toll-like receptor 2 (TLR2), versican and myosin regulatory light chain 2. Immunofluorescence staining for respective markers supported the upregulated levels of Vimentin, myeloperoxidase, immunoglobulin heavy and light chains, J segment (of IgA, IgM), lumican, fibulin 2, and C4a in cyst fluid (Fig. 9). Also, a three-fold increase in matrix metalloproteinase (MMP) 7 and MMP-10 was noted in the cyst fluid. No correlation was found between cyst size and the upregulated proteins ($P > 0.05$).

3.4 Dacryops needling outcomes

Two patients (one male; mean age 50 ± 9.9 years) with palpebral lobe dacryops, measuring 4 × 3 mm, had the dacryops for a mean of 8.2 months (Fig. 9). Patients reported irritation in the eyes and a cystic swelling in the corner of the eye, were using artificial tear drops, and had meibomian gland dysfunction (MGD). Patients were counselled for observation versus intervention for dacryops. An outpatient cyst needling procedure was offered. Follow-up at 8 and 20 weeks revealed no recurrence of cyst. The ductular opening could be appreciated on the slit lamp in one case after cyst aspiration, but not before (Fig. 9). This patient had a bluish tinge around the ductular opening, but no frank enlarged cystic swelling was present.

4 Discussion

The pathogenesis of dacryops has intrigued researchers. As supported by numerous mouse experimental models, the gland is expected to undergo atrophy in response to the blockage of tear ductules [18]. Why does a cyst form and enlarge once the duct is blocked in human lacrimal gland? The current study revealed that inflammation and immune responses are the leading factors in duct ectasia, ductal enlargement, and entrapment of high-molecular-weight proteins, such as complement and immunoglobulins. Another interesting finding was the presence of apolipoproteins in the cyst fluid, indicating the presence of lipids. Lipidomics of the cyst fluid would be needed to understand the lipid composition and its contribution to the pathogenesis of the dacryops. The palpebral lobe of the lacrimal gland is situated in close apposition with the conjunctiva and has foci of immune cells in the conjunctival subepithelial layer overlying the gland lobules [19,20]. The proposed mechanistic theory,

Europe PMC Funders Author Manuscripts

based on the current study findings, is the Inflammatory theory. Once inflammation and fibrosis affect the palpebral lobe conjunctiva, the duct experiences spillover inflammation and blockade of the terminal opening, leading to increased matrix metalloproteinase activity (which can cause ectasia), loss of neural innervation, and accumulation of high-molecular-weight proteins in the cyst cavity. The cyst fluid is rich in immunoglobulins, complement factors, and mucin, which can lead to fluid egress from leaky capillaries into the cyst cavity.

The next question is whether the cyst epithelium is conjunctival or ductular in origin. The cyst epithelium was positive for basal CK15 and superficial CK19 expression, which are expressed in both conjunctival and ductular epithelium as they are ectodermal in origin. The cyst epithelium exhibited squamous metaplasia in two cases and goblet cell metaplasia in one case, a finding also observed in ductular cysts of the salivary glands [21]. There is one report of apocrine metaplasia in dacryops; however, none of the cases in the current series had it [9]. The cyst wall ectasia in the dacryops could be due to MMPs secreted in the inflammatory process. The ectasia of the secreting duct could alter the epithelial activity, as no AQP5 expression was found in the cyst wall. The normal lacrimal gland's secretory ductular epithelium has positivity for AQP5 [22]. It could be due to metaplasia and a change in its secretory phenotype. This was supported by the finding of no difference in AQP5 concentration in the cyst and tear fluid proteomics data (Fig. 9). Based on the current study results, the source of cyst fluid could be the lacrimal gland acini, blood vessels, or active secretion from the cyst epithelium. The cyst is in continuity with normal glandular acini upstream. The upstream uninvolved lobules (not excised with a cyst to preserve the gland) that drain into the dacryops cyst might still be active and contributing to the enlargement of the cyst. We compared the cyst volume and tear secretion rate from the gland ductules. The median tear flow rate per ductule in the human lacrimal gland is 0.25 μL/min [23]. Over 6 months, the cyst volume could have been 65 ml, but the average cyst aspirate volume was 1.4 ml. Hence, upstream acini lobules seem unlikely to be the source of fluid. However, the role of resorption forces cannot be completely ruled out. In dacryops, reactive ectasia of the secreting duct is associated with active chronic inflammation, characterized by the accumulation of fluid and inflammatory molecules, including complement factors and fibulin. The inflammatory process and complement factors can make vessels leaky. The transudation and/or exudation from the increased capillaries in the cyst wall due to the osmotic gradient set by high molecular weight proteins can enlarge the cyst. An increase in proteins involved in the heparin-binding pathway can also cause vessel leakage (Fig. 8). Therefore, a simple cyst aspiration can be considered in patients who are unwilling to undergo surgery. The two cases described in Fig. 9, which underwent simple cyst aspiration, had a good outcome at 8 and 20 weeks. However, the cyst size was not big in these eyes, as the maximum diameter was less than 1 cm. Simple cyst aspiration may not be effective in large-sized dacryops.

The upregulated proteins in the cyst fluid reflect the activity of inflammatory cells found in the cyst wall. Increased neutrophils, plasma cells, and B cells in the cyst wall likely contributed to the elevated levels of myeloperoxidase, MMPs, immunoglobulins, and J segment in the cyst fluid. The upregulated complement pathway proteins belonged to the classical pathway, which is activated by the immunoglobulin-antigen complex. Different immunoglobulin heavy and light chains, as well as J chains (a component of IgA), were

upregulated in the cyst fluid, which again supports the role of the complement pathway in cyst inflammation. Chronic inflammation in the acinar tissue can occur secondary to duct obstruction, as seen in animal models of duct ligation. Duct ligation in mice models increased acinar apoptosis, swelling of acinar cells, dilatation of intralobular ducts, macrophage infiltration by day 5, and fibrosis with loss of acini by day 21 [15]. These experimental models obstruct the main terminal duct of the mice's lacrimal gland, which is the only one in the mice's eyes. The human lacrimal gland has 3 to 5 main terminal ducts that open into the fornix conjunctiva [19]. If one of the ducts gets obstructed, the secretions are still delivered via other ducts; hence, we do not see diffuse acinar fibrosis and loss of acini in dacryops. However, the duct undergoes ectasia and accumulates secretions within the cavity. It is unclear whether the duct stops enlarging at a given time point, as all these cases had palpebral lobe dacryops of similar size. It remains unclear whether every duct obstruction leads to dacryops formation. In the author's practice, many patients have innocuous dacryoliths obstructing the terminal ducts, but no cyst formation occurs in these lacrimal glands because they lack conjunctival inflammation. Perhaps the inciting factor is conjunctival inflammation, which triggers ductal enlargement and fibrosis. In cicatrizing ocular surface inflammatory diseases, such as Stevens-Johnson syndrome, the palpebral lobe conjunctiva exhibits scarring with reduced secretory ducts, without increasing gland size or cyst formation [24,25]. However, exceptions exist, such as giant dacryops cases reported in patients with ocular cicatricial pemphigoid and cicatrizing conjunctivitis [11]. Dacryops can arise from the accessory lacrimal glands, where evidence of tarsal scarring or trachomatous scarring has been reported in many studies [3, 5,7]. Hence, future studies should explore the role of conjunctival inflammation and scarring pathways in inducing dacryops.

An increase in vimentin staining, fibrosis in the cyst wall, upregulated TGF-beta, vimentin protein, and collagen fibrils support the chronic inflammatory process or epithelial-mesenchymal transition (EMT) as a factor contributing to the fibrosis. The lacrimal gland shows EMT in response to injury or duct ligation in a rabbit gland [26]. Expression of other EMT markers, such as Zeb and Snail, is needed to confirm the role of EMT in dacryops. A limitation of the current study is its small sample size. Still, dacryops is a rare condition, and analyzing four samples in detail with proteomics is a novel contribution of this study. The altered protein expression observed in proteomics is supported by immunostaining for IgA + plasma cells, vimentin, fibrosis, macrophages, and lymphocytes. The gene expression profile of dacryops and its comparison with healthy glandular tissue containing ducts would provide further insights into its etiopathogenesis. Additionally, comparing tear proteomics between the two eyes of a patient with unilateral dacryops would reveal the impact of cyst formation on tear film dynamics.

Based on the current study results, inflammation and ductal obstruction, accompanied by increased metalloproteinase and immunoglobulin levels, indicate that the classical complement pathway contributes to dacryops development. A loss of neural plexus in the cyst wall is observed, which could be secondary to inflammation but requires confirmation in future studies. Future studies should also perform lipidomics on the cyst fluid and evaluate gene expression to further understand the etiopathogenesis of ductular cysts.

Acknowledgment

The author thanks Mr. Tirupathi Rao for his contributions to histological and immunofluorescence staining. The contributions of ocular pathologist, Dr Dilip Kumar Mishra, Ophthalmic Pathology Laboratory, LV Prasad Eye Institute, in are duly acknowledged. The author (S.S) is an India Alliance DBT/Wellcome Trust early career fellow, and the current research is funded by the same agency (IA/CPHE/21/1/505970).

References

[1]. Bullock JD, Fleishman JA, Rosset JS. Lacrimal ductal cysts. Ophthalmol. 1986; 93: 1355–60. [PubMed: 3785895]

[2]. Lam K, Brownstein S, Jordan DR, Jastrzebski A. Dacryops: a series of 5 cases and a proposed pathogenesis. JAMA Ophthalmol. 2013; Jul; 131 (7) 929–32. [PubMed: 23846204]

[3]. Weatherhead RG. Wolfring dacryops. Ophthalmol. 1992; Oct; 99 (10) 1575–81. [PubMed: 1454325]

[4]. Jakobiec FA, Zakka FR, Perry LP. The cytologic composition of dacryops: an immunohistochemical investigation of 15 lesions compared to the normal lacrimal gland. Am J Ophthalmol. 2013; Feb; 155 (2) 380–396. e1 [PubMed: 23114708]

[5]. Smith S, Rootman J. Lacrimal ductal cysts: presentation and management. Surv Ophthalmol. 1986; 30 (4) 245–50. [PubMed: 3952646]

[6]. Tanaboonyawat S, Idowu OO, Copperman TS, Vagefi MR, Kersten RC. Dacryops - a review. Orbit. 2020; Apr; 39 (2) 128–34. [PubMed: 31512543]

[7]. Galindo-Ferreiro A, Alkatan HM, Muinos-Diaz Y, Akaishi PM, Galvez-Ruiz A, Cruz AV. Accessory lacrimal gland duct cyst: 23 years of experience in the Saudi population. Ann Saudi Med. 2015; Sep-Oct; 35 (5) 394–9. DOI: 10.5144/0256-4947.2015.394 [PubMed: 26506974]

[8]. Ozgonul C, Uysal Y, Ayyildiz O, Kucukevcilioglu M. Clinical features and management of dacryops. Orbit. 2018; Aug; 37 (4) 262–5. [PubMed: 29300516]

[9]. Kacerovska D, Michal M, Ricarova R, Frdlikova D, Sosna B, Kazakov DV. Apocrine secretion in lacrimal gland cysts (dacryops): a common but underrecognized phenomenon. J Cutan Pathol. 2011; Sep; 38 (9) 720–3. [PubMed: 21752047]

[10]. Mudhar HS, Currie ZI, Salvi SM. Lacrimal gland intra-lobular duct cysts associated with focal vasculitis. Ocul Oncol Pathol. 2015; Jun; 1 (4) 225–30. DOI: 10.1159/000375255 [PubMed: 27354982]

[11]. Remulla HD, Rubin PA. Giant dacryops in a patient with ocular cicatricial pemphigoid. Br J Ophthalmol. 1995; Nov; 79 (11) 1052–3. DOI: 10.1136/bjo.79.11.1052 [PubMed: 8534655]

[12]. Salam A, Barrett AW, Malhotra R, Olver J. Marsupialization for lacrimal ductular cysts (dacryops): a case series. Ophthalmic Plast Reconstr Surg. 2012; Jan-Feb; 28 (1) 57–62. [PubMed: 21956544]

[13]. Kurup SP, Lissner GS. Characterization of dacryops infections. Ophthalmic Plast Reconstr Surg. 2015; Jan-Feb; 31 (1) 58–62. [PubMed: 24892277]

[14]. Alsarhani WK, Al-Sharif EM, Al-Faky YH, Alkatan HM, Maktabi AM, Alsuhaibani AH. Dacryops and clinical diagnostic challenges. Can J Ophthalmol. 2022; Dec; 57 (6) 388–93. [PubMed: 34324876]

[15]. He X, Wang S, Sun H, He H, Shi Y, Wu Y, Wu H, Liu Z, Zhuang J, Li W. Lacrimal gland microenvironment changes after obstruction of lacrimal gland ducts. Investig Ophthalmol Vis Sci. 2022; Mar 2. 63 (3) 14. doi: 10.1167/iovs.63.3.14 [PubMed: 35289845]

[16]. Singh S, Ali MJ. Is orbital lobe of the lacrimal gland dispensable? Tear volume, ocular surface, and MRI volumetric analysis. Ophthalmic Plast Reconstr Surg. 2025; 41 (3) 285–8. DOI: 10.1097/IOP.0000000000002815 [PubMed: 39329296]

[17]. Singh S, Rao BS, Basu S. Altered prostaglandin E receptor subtype 3 expression in lacrimal glands of patients with chronic Stevens-Johnson syndrome. Ocul Immunol Inflamm. 2023; Feb; 31 (2) 343–7. [PubMed: 35113749]

[18]. Perschbacher K, Jackson-Boeters L, Daley T. The adhesion molecules NCAM, HCAM, PECAM-1 and ICAM-1 in normal salivary gland tissues and salivary gland malignancies. J Oral Pathol Med. 2004; Apr; 33 (4) 230–6. [PubMed: 15061711]

[19]. Singh S, Basu S. The human lacrimal gland: historical perspectives, current understanding, and recent advances. Curr Eye Res. 2020; Oct; 45 (10) 1188–98. [PubMed: 32450044]

[20]. Singh S, Winter Z, Necker F, Bäuerle T, Scholz M, Bräuer L, Paulsen F. New insights into lacrimal gland anatomy using 7T MRI and electron microscopy: relevance for lacrimal gland targeted therapies and bioengineering. Ocul Surf. 2023; Oct. 30: 204–12. [PubMed: 37774917]

[21]. Stojanov IJ, Malik UA, Woo SB. Intraoral salivary duct cyst: clinical and histopathologic features of 177 cases. Head Neck Pathol. 2017; Dec; 11 (4) 469–76. DOI: 10.1007/s12105-017-0810-5 [PubMed: 28349371]

[22]. Fu L, Zhao Z, Zhao S, Zhang M, Teng X, Wang L, Yang T. The involvement of aquaporin 5 in the inflammatory response of primary sjogren's syndrome dry eye: potential therapeutic targets exploration. Front Med. 2024; Sep 23. 11 1439888 doi: 10.3389/fmed.2024.1439888 [PubMed: 39376655]

[23]. Singh S, Shanbhag SS, Basu S. Tear secretion from the lacrimal gland: variations in normal versus dry eyes. Br J Ophthalmol. 2022; Jun; 106 (6) 772–6. [PubMed: 33597197]

[24]. Singh S, Basu S. Large dacryops with an ectopic lacrimal ductule following membranous conjunctivitis. Indian J Ophthalmol. 2023; May; 71 (5) 2267–8. DOI: 10.4103/IJO.IJO_2624_22 [PubMed: 37202967]

[25]. Singh S, Shanbhag SS, Basu S. Palpebral lobe of the human lacrimal gland: morphometric analysis in normal versus dry eyes. Br J Ophthalmol. 2021; Oct; 105 (10) 1352–7. [PubMed: 32920529]

[26]. Singh S, Brabletz S, Arnold P, Schicht M, Paulsen F. Epithelial-mesenchymal transition in the lacrimal gland morphogenesis, damage and repair. Ocul Surf. 2023; 29: 401–5. [PubMed: 37321448]

[27]. Yuksel S, Kumar P, Krenz SE, et al. Aging Affects Lipid Homeostasis in Lacrimal Glands by Upregulating Lipogenesis and Changing Its Specificity. Invest Ophthalmol Vis Sci. 2025; 66 (13) 1. doi: 10.1167/iovs.66.13.1 [PubMed: 41031741]

Europe PMC Funders Author Manuscripts

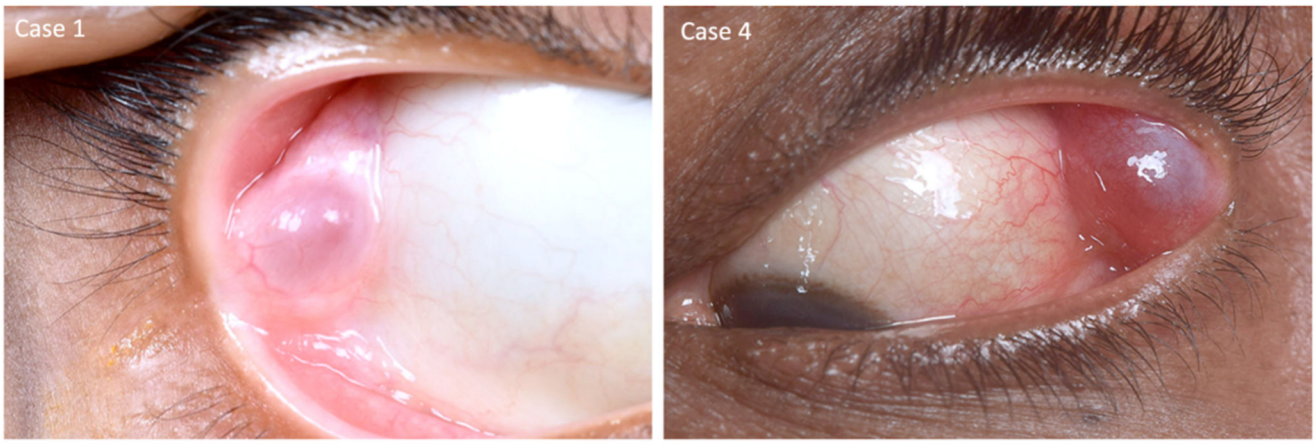

Fig. 1. A & B, Dacryops arising from the palpebral lobe of the lacrimal gland seen in Cases 1 & 4.

Case 4 has an inflamed overlying conjunctival epithelium.

Europe PMC Funders Author Manuscripts

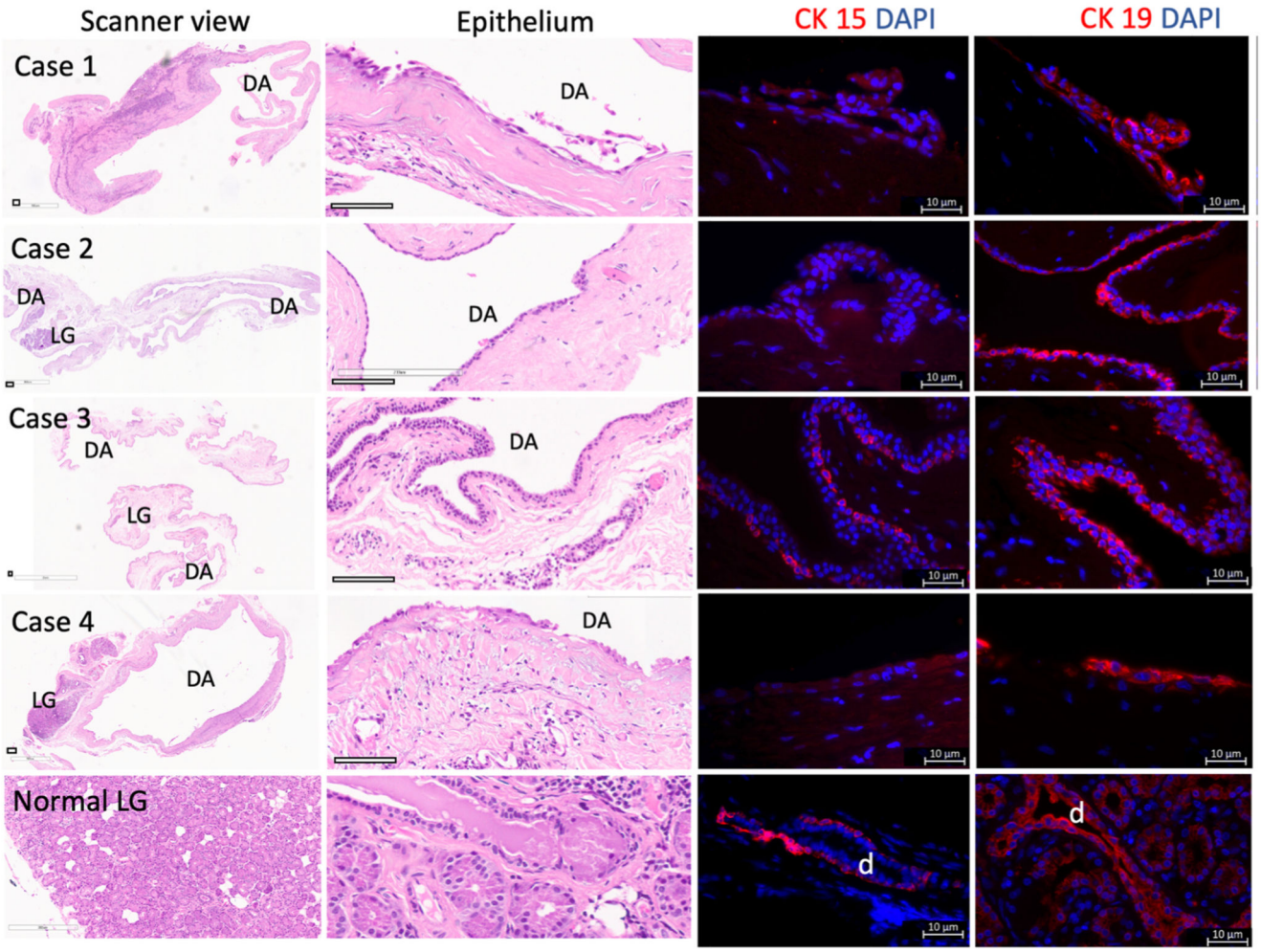

Fig. 2. Hematoxylin & eosin, Cytokeratin 15, 19, staining of four dacryops specimens

(scale bar represents 10 µm). The first column shows the scanner view, which shows the cyst wall, the dacryops (DA) lumen, and the visible lacrimal gland (LG) within specimens at very low magnification. The second column shows the cyst epithelial lining as a two-layered cuboidal epithelium in cases 1 to 3. The third column shows basal CK15 positivity in only case 3, whereas CK19 positivity is seen in all epithelial layers of all specimens. The normal lacrimal gland (last row) shows positive CK15 expression in the basal ductal (d) epithelial cells, whereas CK19 expression is positive in acinar epithelial cells.

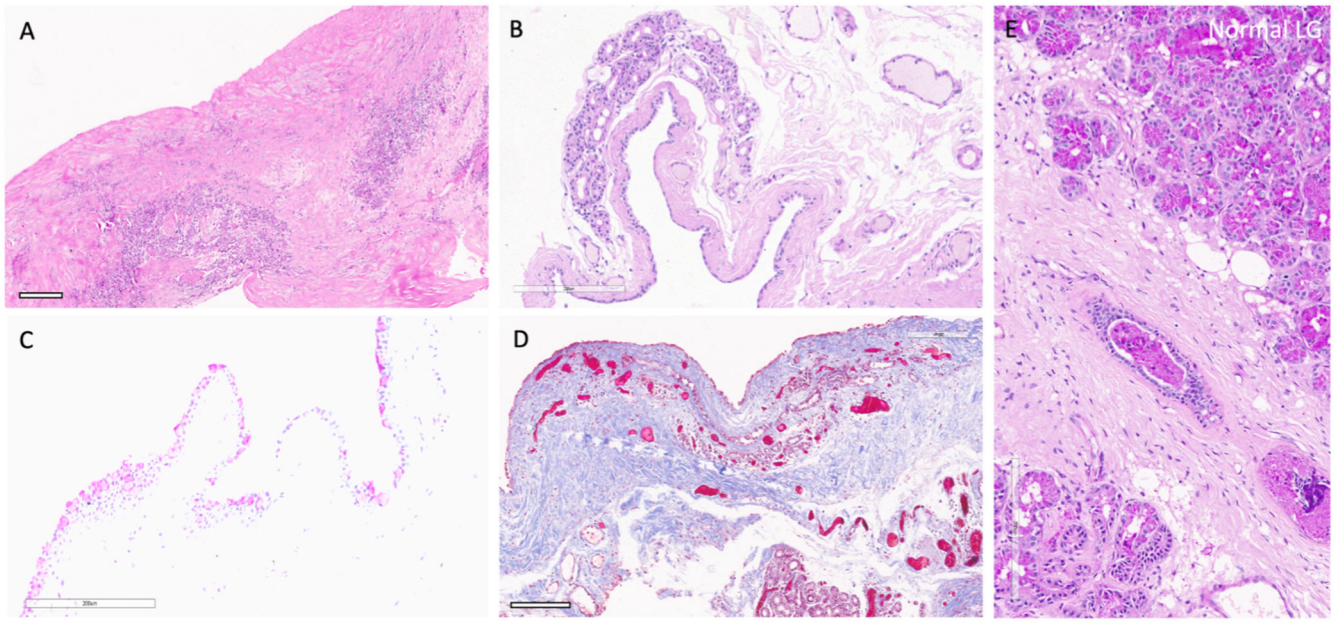

Fig. 3. PAS staining of four dacryops specimens shows positive goblet cells in case 3 only, and the normal lacrimal gland (E) lacks any goblet cells in the ductal epithelium.

PAS-positive granules are seen in the cytoplasm of acinar epithelial cells.

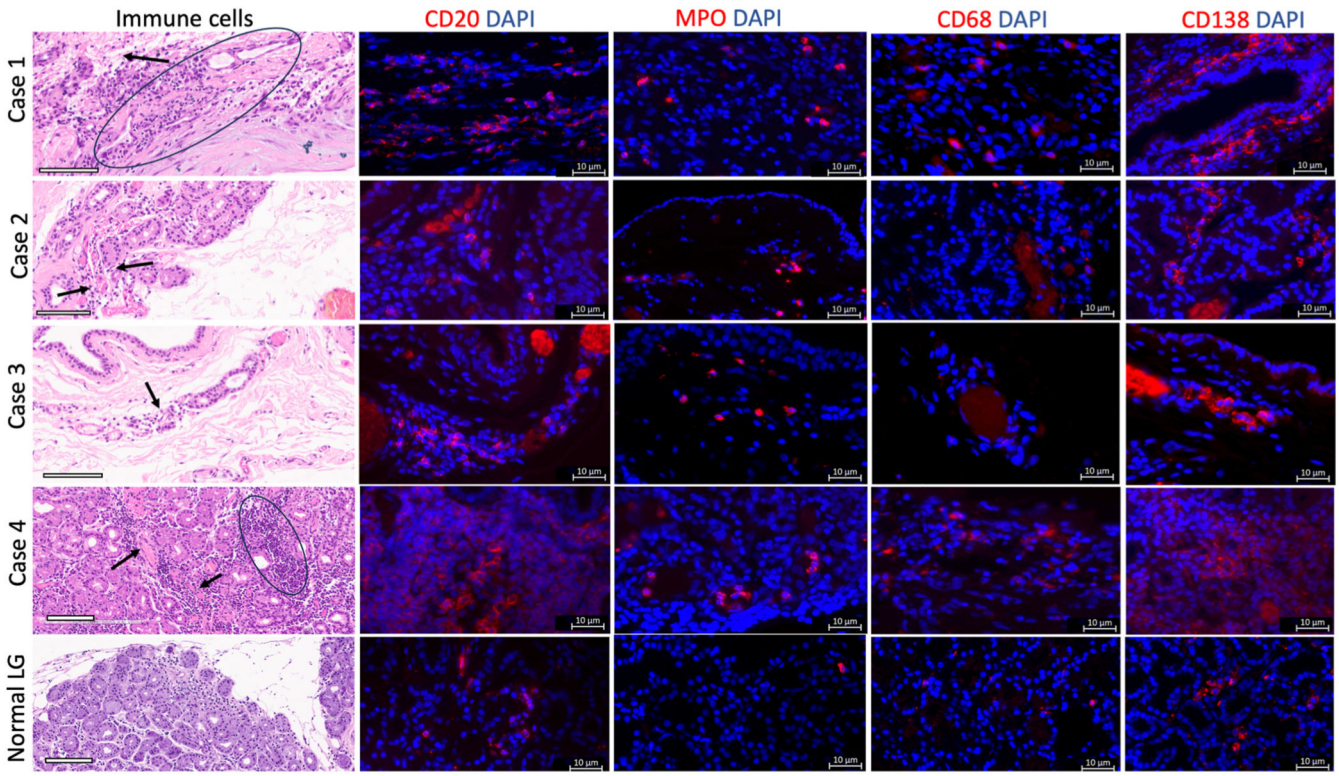

Fig. 4. Inflammatory cell expression stained with CD20, CD138, myeloperoxidase, and CD68 antibodies in four dacryops specimens

(scale bar represents 10 μm). The first column shows the H&E-stained specimens with scattered immune cells (marked with an arrow) infiltrating the glandular acini, mainly in perivascular locations. The second column shows CD20-positive B lymphocytes in all specimens. In the third and fourth columns, a few stromal cells are positive for MPO and CD68 markers, indicating neutrophils and macrophages. The fifth column shows the CD138-positive cells in the subepithelial and acinar stroma. The normal lacrimal gland (last row) shows few scattered CD20, CD68, and CD138-positive cells in the glandular stroma, whereas MPO is negative within the gland.

Europe PMC Funders Author Manuscripts

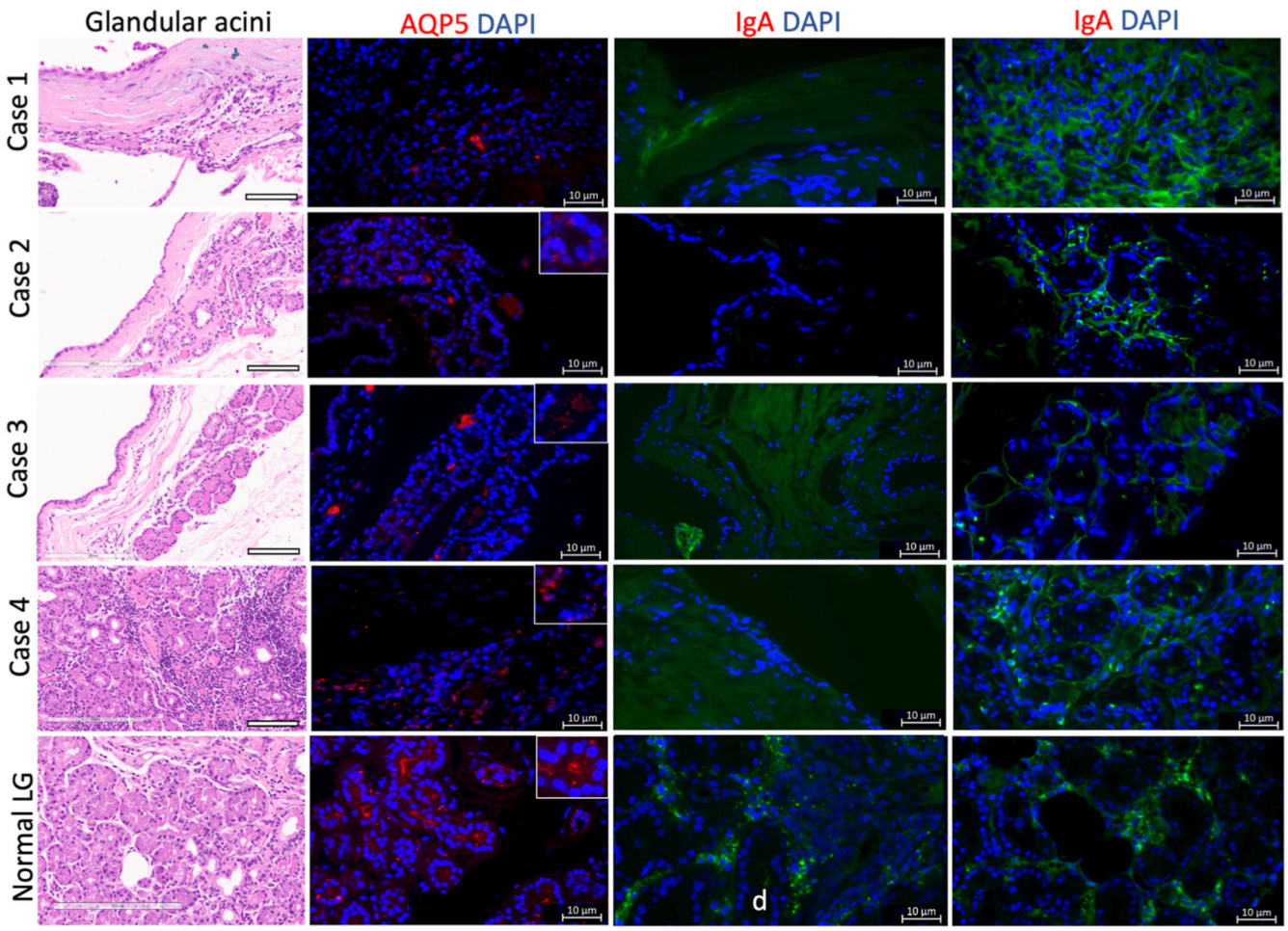

Fig. 5. AQP5, IgA expression in visible lacrimal gland acini in dacryops specimens

(scale bar represents 10 µm). The first column shows the H&E-stained specimens, with visible glandular acini in cases 2 to 4; however, no acinar tissue was observed in Case 1. The second column shows AQP5 expression as cytoplasmic in Cases 2 & 4 (inset shows perinuclear staining), whereas it is membranous in Case 3 (inset shows positivity towards the acinar lumen). No AQP5 expression was seen in cyst epithelium. The third column shows absent IgA expression in cyst epithelium or the subepithelial region. The fourth column shows positive IgA expression within interstitial cells in cases 2 & 4, likely plasma cells interspersed between acini. The normal lacrimal gland (last row) shows membranous AQP5 positivity in acinar epithelial cells, whereas IgA-positive plasma cells are seen interspersed between acini and periductal (d) space.

Europe PMC Funders Author Manuscripts

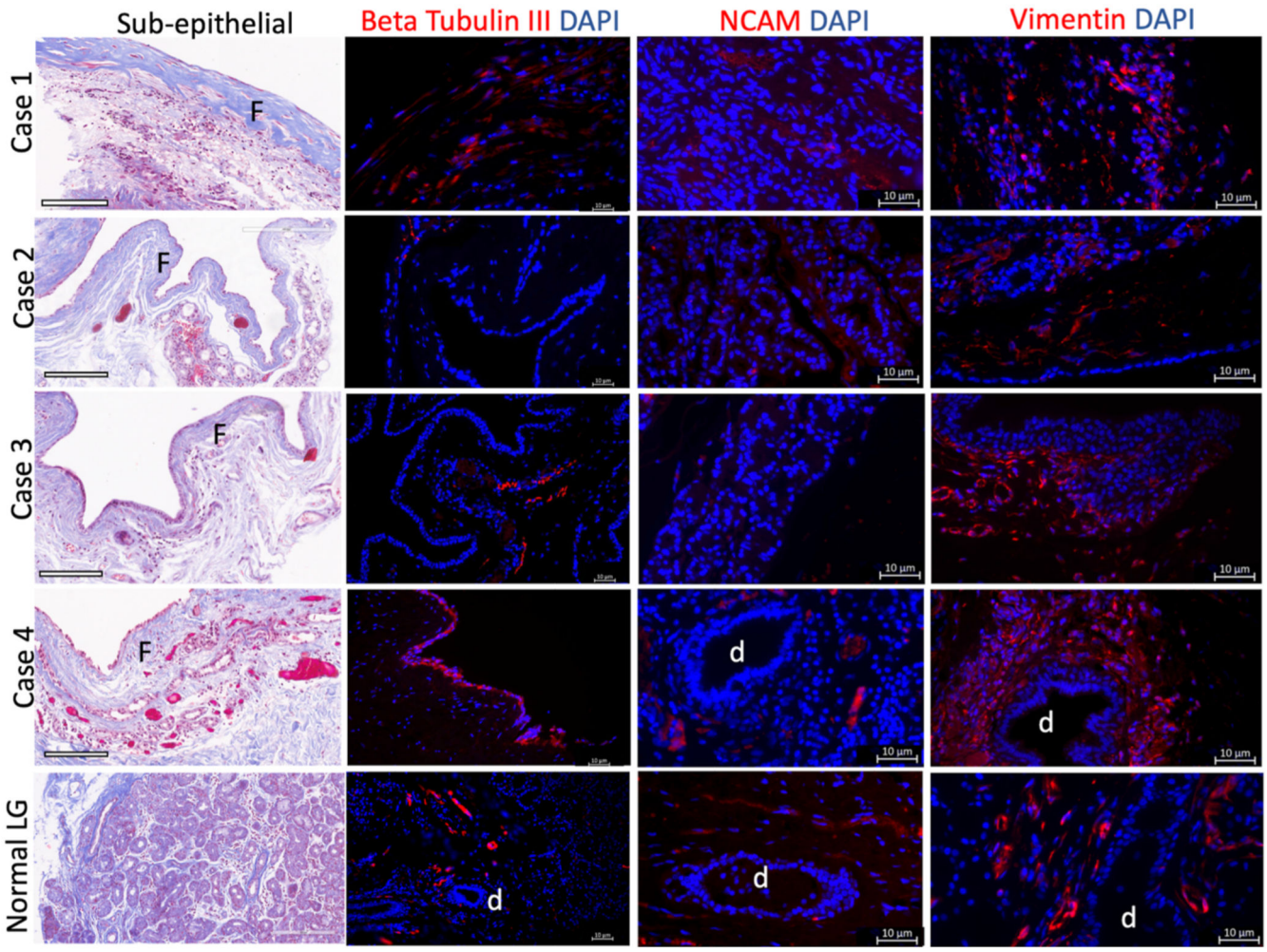

Fig. 6. Neural and stromal marker expression in four dacryops specimens

(scale bar represents 10 µm). The first column shows bluish fibrotic regions on Masson-trichrome staining in subepithelial and stromal areas. The second column shows positive beta-tubulin staining in the scattered stromal cells, but it is missing from the subepithelial or basal epithelial layers. The third column shows absent NCAM expression in acini or stromal cells. The fourth column shows vimentin positivity in spindle-shaped fibroblasts, mononuclear immune cells, likely lymphocytes, and endothelial cells of capillaries. The normal lacrimal gland (last row) shows Masson-trichrome positive interstitium and beta-tubulin and NCAM-positivity in periacinar and periductal (d) areas.

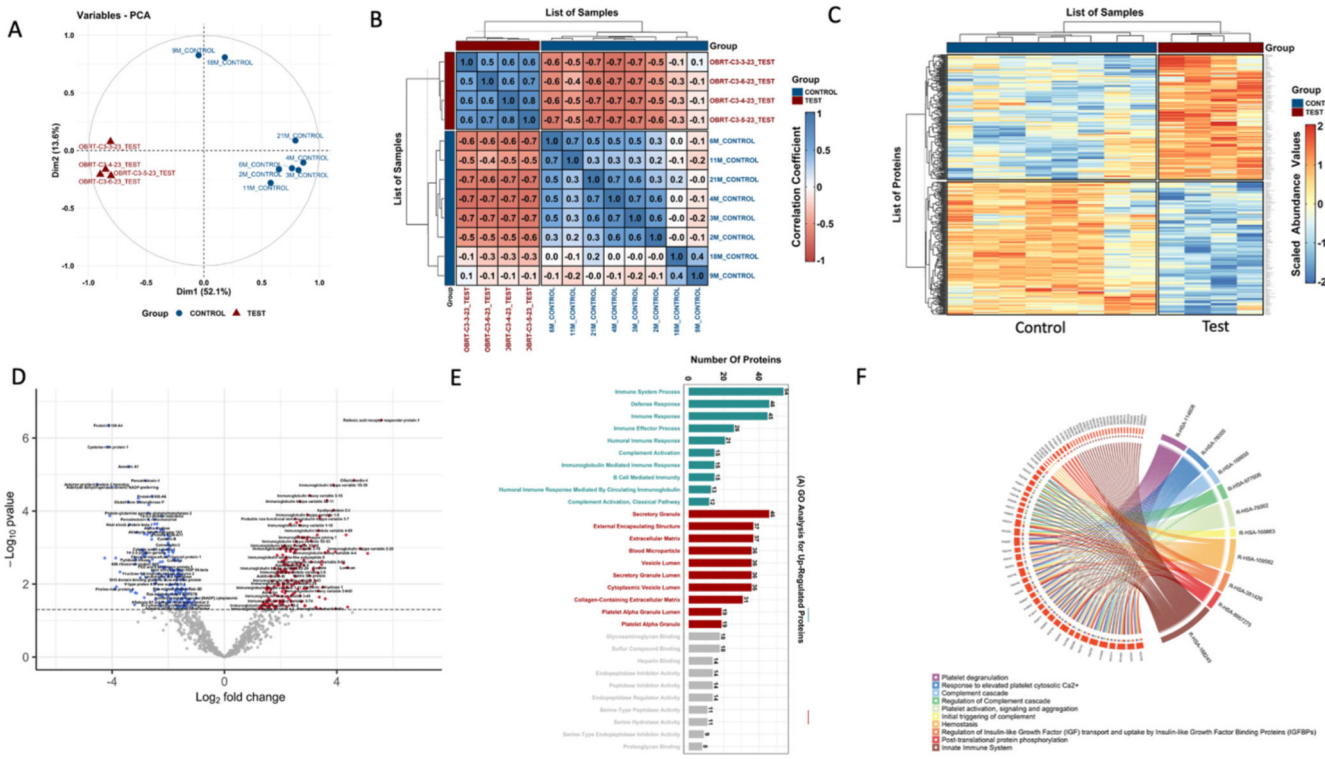

Fig. 7. A, Principal coordinate analysis shows wide separation between cyst fluid (test) and tear samples (control).

The correlation plot showed a negative correlation between the samples. Heat map (C) and volcano plot showed differentially expressed proteins in the two samples (D). Gene ontology pathway analysis (E) shows the number of proteins involved in upregulated pathways related to biological process, metabolism, and cellular components. F, Chord diagram showing the innate immune system to have the widest arc and the most extended chords among the identified proteins in upregulated pathways.

Europe PMC Funders Author Manuscripts

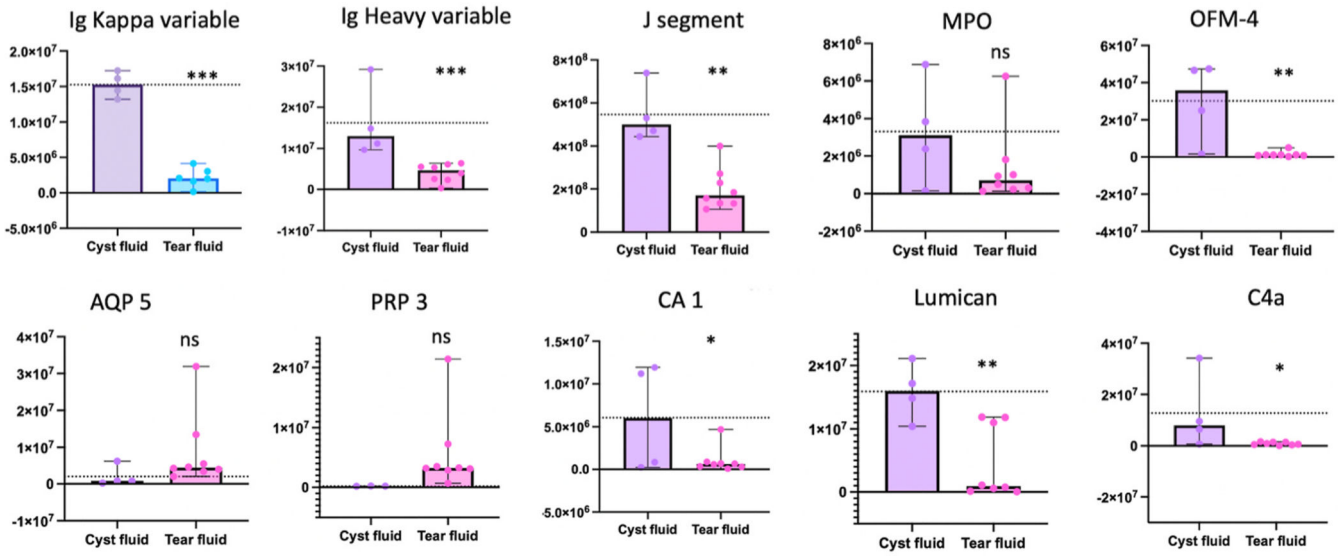

Fig. 8. Raw abundance values of different proteins compared between cyst and tear fluid.

Proteins- Immunoglobulin kappa variable, Immunoglobulin heavy variable, J segment, Myeloperoxidase (MPO), Olfactomedin-4 (OLFM-4), Aquaporin 5 (AQP), Proline-rich protein 3 (PRP 3), Carbonic anhydrase 1 (CA1), Lumican, Complement factor 4a. *P < 0.05, **P < 0.01, ***P < 0.001.

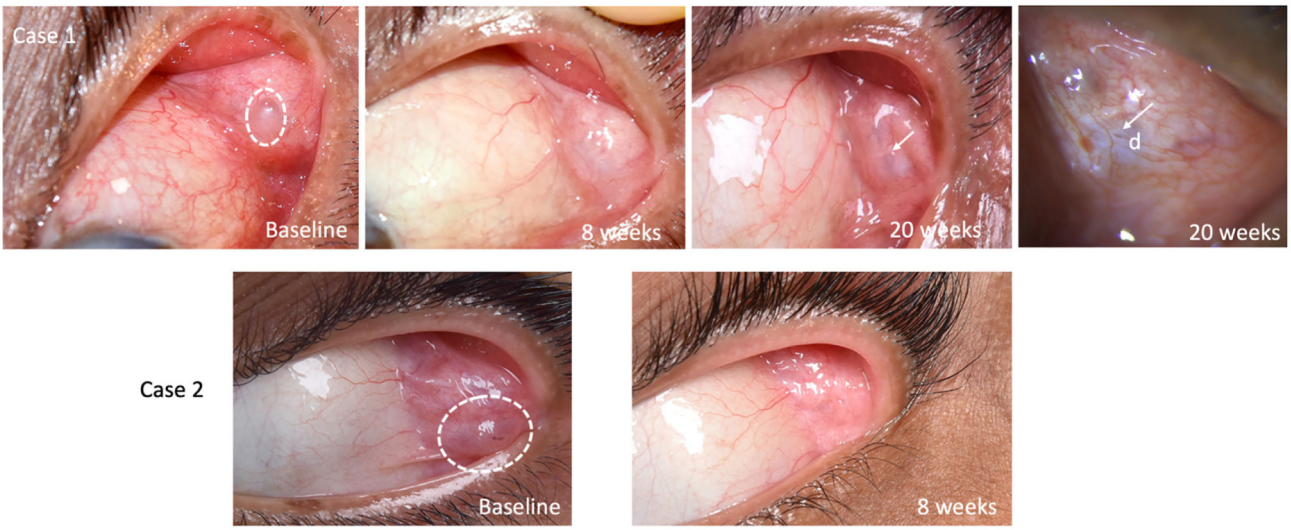

Fig. 9. First row shows external photographs of left palpebral lobe dacryops (marked with a dashed circle) in an adult male that resolved at 8- and 20-week post-needle evacuation of cyst contents.

Slit-lamp photo at 20 weeks shows slit-shaped ductular (d) opening in the area of dacryops (marked with an arrow). The second row shows another female patient with left dacryops in the palpabral lobe (marked with a dashed circle) that resolved at 8-week follow-up after needling.

Europe PMC Funders Author Manuscripts

Table 1 Summary of histopathological and immunostainig results in four dacryops specimens.

Case no. (Age/ Sex)	Cyst Epithelium	Apical snout formation	Inflammation*	Lacrimal gland acini	Mucus-secreting goblet cells	Vimentin	CD20	CD3	CD68	MPO	Beta 3 Tubulin in epithelium
1 (57/F)	squamous to cuboidal	−	++	−	−	+, fibroblast, macrophages	++	−	+	+	−
2 (43/ M)	Cuboidal to columnar	+	+	+	−	+, fibroblast, macrophages	+	−	+	+	−
3 (16/ M)	Cuboidal to columnar	+	+	+	+	+, fibroblast, macrophages	+	−	+	+	−
4 (53/ M)	Cuboidal to columnar	+	++	+	−	+, fibroblast, macrophages	++	−	++	+	−

Europe PMC Funders Author Manuscripts

Table 2 Summary of immunostaining results within the lacrimal gland acini seen in three specimens.

Case no. (Age/Sex)	AQP5 expression[a]	Beta 3 tubulin	NCAM	IgA expression in acini	IgA expression in cyst epithelium
2 (43/M)	Acini	+, stroma	+, stroma	+	−
3 (16/M)	Acini	+, stroma	+, stroma	−	−
4 (53/M)	Acini	++, epithelium & stroma	+, stroma	+	−

AQP 5 = Aquaporin 5; NCAM= Neural cell adhesion molecule.

[a]AQP5 expression noted in acinar cells only and not in cyst epithelium.

Europe PMC Funders Author Manuscripts

Table 3 List of top 20 upregulated proteins in cyst fluid along with log fold change and significance value.

Protein description	Log fold change	P value
Retinoic acid receptor responder protein 1	5.584	0.0000007
Immunoglobulin heavy variable 3-35	5.099	0.001
Immunoglobulin kappa variable 2-28	4.851	0.001
Olfactomedin-4	4.608	0.00001
Mannosyl-oligosaccharide 1,2-alpha-mannosidase IA	4.385	0.042
Lumican	4.376	0.003
Podocalyxin	4.326	0.000
Fibulin-2	4.238	0.002
Hemoglobin subunit alpha	3.953	0.047
Leucine-rich repeat protein 1	3.949	0.001
Apolipoprotein C-I	3.884	0.00009
Immunoglobulin kappa variable 1D-39	3.874	0.00001
Complement C4a	3.723	0.0001
Matrilysin	3.684	0.001
Apolipoprotein E	3.652	0.00005
Immunoglobulin heavy variable 2-70D	3.584	0.025
Immunoglobulin heavy variable 4-4	3.574	0.001
Carbonic anhydrase 1	3.509	0.012
Chitinase-3-like protein 1	3.469	0.002
Mucin-5B	3.455	0.003